Contribution of Buried Lysine Residues to the Oligomerization Specificity and Stability of the Fos Coiled Coil†

Kathleen M. Campbell,‡ Aaron J. Sholders,‡ and Kevin J. Lumb*,‡,§

Department of Biochemistry and Molecular Biology and Department of Chemistry, Colorado State University, Fort Collins, Colorado 80523-1870

Received November 9, 2001; Revised Manuscript Received January 17, 2002

ABSTRACT: Coiled coils comprise two or more helices characterized by a heptad repeat of amino acids denoted a through g. The buried a and d positions are usually occupied by hydrophobic residues. Fos dimerizes via a coiled coil (leucine zipper) with Jun family members to form the transcription factor AP-1. Fos homodimers are relatively unstable due to unfavorable interhelical electrostatic interactions within the Fos two-stranded coiled coil. The Fos coiled coil contains two polar position a Lys residues (Lys 16 and Lys 30 of Fos-p1, a peptide corresponding to the coiled-coil domain of v-Fos). Lys 16 and Lys 30 of Fos-p1 were replaced individually and together with the unnatural amino acid norleucine (2-aminohexanoic acid), which corresponds to a deletion of the Lys ϵ-amino group. The midpoint of thermal denaturation (T_m) of Fos-p1 (10 μM) is 30 °C at pH 7. The Lys 16 → Nle variant forms predominantly homodimers that are relatively unstable (T_m = 46 °C). The Lys 30 → Nle variant forms a stable homotetramer (T_m = 60 °C). The Lys 16/Lys 30 → Nle variant forms a very stable homotetramer (T_m = 80 °C). The results show that (i) the effects of buried position a Lys residues on coiled-coil oligomerization are context dependent and (ii) electrostatic destabilization of the Fos homodimer can be mitigated by an oligomerization switch moderated by a single buried Lys residue.

The coiled coil governs protein−protein interactions in a diverse range of structural and regulatory proteins (*1*, *2*). The motif is widespread in natural proteins, with over 5% of putative open reading frames of sequenced genomes predicted to contain coiled coils (*3*). Coiled coils consist of two or more helices that assemble with either a parallel or antiparallel orientation (*1*, *2*). The hallmark sequence feature of the coiled coil is a heptad repeat of seven amino acids labeled a through g containing a repeat of usually hydrophobic amino acids at positions a and d (*4*, *5*). The hydrophobic interface between the helices of a coiled coil comprises residues at positions a, d, e, and g (*6*−*8*). Residues at the e and g positions are often charged (*4*, *5*, *9*−*15*) and may participate in interhelical electrostatic interactions (*4*, *5*, *16*).

A classic example of a parallel, coiled-coil heterodimer is the leucine zipper of the Fos−Jun transcription factor (AP-1)[1] (*17*, *18*). AP-1 is implicated in cellular processes such as differentiation, oncogenesis, and apoptosis (*19*−*21*). The dimerization specificity of the Fos−Jun heterodimer is embodied in the leucine zipper coiled-coil domain (*17*). Jun can form a stable homodimer (*19*). In contrast, the Fos homodimer is destabilized by unfavorable interhelical electrostatic interactions between Glu residues at e and g′ positions in the leucine zipper of the Fos homodimer (Figure 1A) (*22*−*24*). These unfavorable interactions are relieved upon heterodimerization with Jun, and so the specificity of Fos−Jun heterodimerization is driven by the instability of the Fos homodimer (*23*).

Four of the five a positions of the Fos leucine zipper are occupied by either charged (Lys) or neutral polar (Thr) amino acids (Figure 1A). These positions are usually, but not exclusively, occupied by hydrophobic amino acids (*4*, *5*, *9*−*15*). Buried polar residues at a positions of coiled coils can dictate coiled-coil oligomerization and helix orientation (*6*, *7*, *25*−*35*). Position a Lys residues have been observed to impart dimerization specificity (*28*) and to occur more frequently in two-stranded than in three-stranded coiled coils (*10*, *13*, *15*). Simultaneous replacement of four or five of the polar position a residues of the Fos leucine zipper with hydrophobic amino acids results in Fos mutants that activate transcription in vivo, which was interpreted to result from the formation of stable homodimers by the Fos mutants (*36*).

We show here that the electrostatic mechanism of Fos destabilization can be overcome by an oligomerization switch of the Fos leucine zipper that is mediated by one of the two position a Lys residues of Fos. The effects of the two position a Lys residues on oligomerization are different and so depend on context. The results extend our understanding of the basis

† Supported by the donors of the Petroleum Research Fund, Grant 35760-AC4, administered by the American Chemical Society, and NIH Equipment Grant RR11847. K.M.C. was supported in part by a Colorado Institute for Research in Biotechnology Fellowship. A.J.S. was supported in part by NSF Research Experiences for Undergraduates Grant DBI-9820175.

* Corresponding author. E-mail: lumb@lamar.colostate.edu.

‡ Department of Biochemistry and Molecular Biology.

§ Department of Chemistry.

[1] Abbreviations: [θ], molar ellipticity; $[\theta]_{222}$, molar ellipticity at 222 nm; ANS, 1-anilinonaphthalene-8-sulfonic acid; AP-1, activating protein 1; CD, circular dichroism; HPLC, high-performance liquid chromatography; Nle, norleucine (2-aminohexanoic acid); PBS, phosphate-buffered saline (10 mM sodium phosphate and 150 mM NaCl); T_m, midpoint of thermal denaturation.

10.1021/bi0159276 CCC: $22.00
Published on Web 03/20/2002

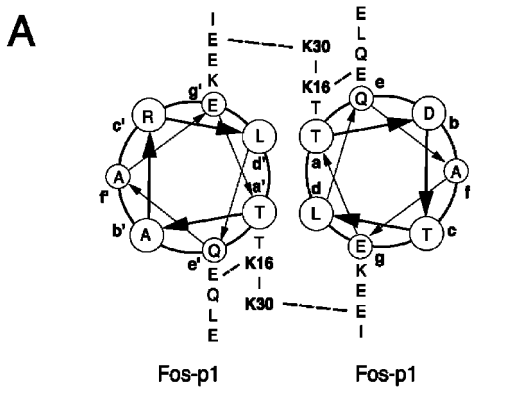

FIGURE 1: (A) Helical wheel representation of the Fos−Fos leucine zipper, shown as a parallel, two-stranded coiled coil (*17*). A view down the helix from the amino terminus is shown. The d position residues are all Leu and are omitted after the first heptad for clarity, as are the b, c, and f position residues. Putative intra- and interhelical polar interactions involving Lys 16 and Lys 30 (shown in bold) are indicated with dashed lines. (B) Amino acid sequence of Fos-p1 (*17*). The N-terminus is acetylated, and the C-terminus is amidated.

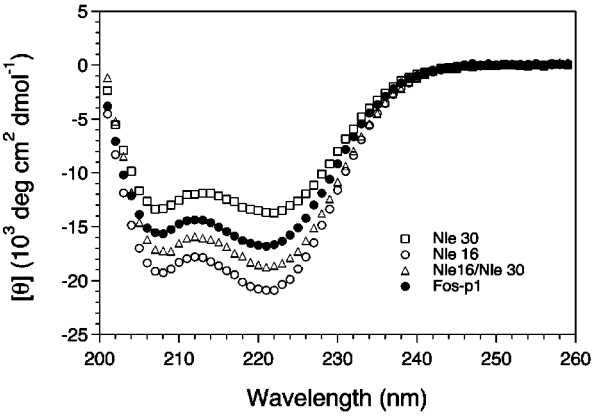

FIGURE 2: CD spectra of Fos-p1 and the Lys 16 → Nle, Lys 30 → Nle, and Lys 16/Lys 30 → Nle variants at 5 °C (PBS, pH 7.0, total peptide concentration 10 μM). The minima at 208 and 222 nm indicate that the peptides form helical structures. The origin of the different magnitudes of the CD spectra is unclear (see Results) but does not simply reflect changes in the fraction of globally unfolded peptide. Each peptide exhibits a folded baseline during thermal unfolding (Figure 3), implying that the peptides are not in equilibrium between fully folded and fully unfolded states at the low temperature (5 °C) of the wavelength scans (*46*).

of Fos−Jun assembly, in that electrostatic destabilization of Fos association relies on dimerization, and illustrate the importance of considering context when using position a Lys residues as a sequence feature for identifying dimeric coiled coils.

EXPERIMENTAL PROCEDURES

Peptides with acetylated N-termini and amidated C-termini were synthesized on MBHA (4-methylbenzhydrylamine hydrochloride salt) resin (100−200 mesh) with manual Boc chemistry (*37*). The following protecting groups were used: Asn(Xan), Asp(Bzl), Gln(Xan), Glu(Bzl), Lys(2-Cl-Z), Ser-(Bzl) Thr(Bzl), and Tyr(Bzl). Peptides were purified by C_{18} HPLC using linear water/acetonitrile gradients containing 0.1% (v/v) trifluoroacetic acid. The identity of each peptide was confirmed with MALDI mass spectrometry, and in all cases the expected and observed masses agreed to within 1 Da.

Concentrations of peptide stock solutions were determined by Tyr absorbance in 6 M GuHCl, 10 mM sodium phosphate, and 50 mM NaCl, pH 6.5, using an extinction coefficient at 276 nm of 1450 cm^{-1} M^{-1} (*38*).

CD spectroscopy was performed with an Aviv 202 spectrometer. Samples contained 10 μM peptide in PBS (10 mM sodium phosphate and 150 mM NaCl), pH 7.0. Thermal stability was monitored from the change in $[\theta]_{222}$ with temperature. The temperature was increased in steps of 2 °C with an equilibration time of 60 s. The CD signal at 222 nm was averaged over 60 s. The T_m was determined from the maxima of the first derivative of $[\theta]_{222}$ with T $(K)^{-1}$ (*39*).

Sedimentation equilibrium experiments were performed with a Beckman XL-I analytical ultracentrifuge. Samples were dialyzed for at least 12 h against the reference buffer (PBS, pH 7.0). Data were collected at 5 °C at 35, 40, and 45 krpm on samples of initial loading concentrations of 70 and 140 μM using two-sector centerpieces. Peptide concentrations spanned approximately 20−700 μM at equilibrium. Sapphire windows were used, which alleviated apparent sticking of the Fos peptides to quartz windows. A directly measured solvent density of 1.008 g mL^{-1} and calculated partial specific volumes of 0.744 mL g^{-1} (Fos-p1), 0.745 mL g^{-1} (single Nle variants), and 0.747 mL g^{-1} (double Nle variant) were used (*40*). Data were fit using ORIGIN (Beckman Instruments) to single-species and self-associating models both as individual data sets and as a global fit of all six data sets for each peptide. The validity of different models was evaluated by the distribution of residuals and the variance. Results are reported as the mean mass of the individual data sets ± the standard error and as the mass and variance obtained from global fits.

ANS binding was monitored at 5 °C with an Aviv ATF105 fluorometer. Emission spectra were collected from 290 to 600 nm using an excitation wavelength of 355 nm. Samples contained 10 μM peptide and 1 μM ANS (Molecular Probes) in PBS, pH 7.0. ANS concentration was determined for a stock solution in methanol by absorbance at 372 nm using an extinction coefficient of 7.8×10^3 cm^{-1} M^{-1}.

RESULTS

Fos-p1 (Figure 1B) corresponds to the leucine zipper region of v-Fos (residues 161−200) and is identical to the leucine zipper of human c-Fos with the exception of a single g position amino acid substitution; Glu 175 of human c-Fos is substituted with Lys in v-Fos (*41*). Although Fos-p1 forms a helical dimer at micromolar concentrations, the dissociation constant for dimerization (approximately 5.6 μM at 25 °C, pH 7) precludes dimerization at nanomolar concentrations (*17*).

To evaluate the contribution of position a polar Lys residues to the formation of the Fos leucine zipper, Lys 16 and Lys 30 were substituted separately and together with the unnatural amino acid norleucine (Nle, 2-aminohexanoic acid). This substitution corresponds to a deletion of the side chain ϵ-amino moiety of Lys while leaving the remainder of the hydrophobic side chain intact. Lys 16 and Lys 30 of Fos-p1 correspond to Lys 176 and Lys 190, respectively, of full-length human c-Fos and v-Fos (*41*).

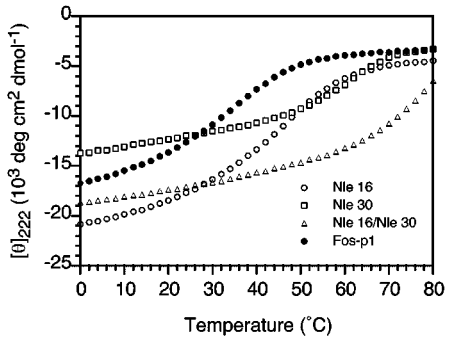

FIGURE 3: Temperature dependence of $[\theta]_{222}$ for Fos-p1 ($T_m = 30$ °C) and the Lys 16 → Nle ($T_m = 46$ °C), Lys 30 → Nle ($T_m = 60$ °C), and Lys 16/Lys 30 → Nle ($T_m = 80$ °C) variants (PBS, pH 7.0, total peptide concentration 10 μM).

Table 1: ANS Binding Properties of the Fos-p1 and Variant Peptides[a]

	λ_{max} (nm)	relative fluorescence intensity at λ_{max}
ANS, pH 7.0	500	1.0
α-lactalbumin molten globule, pH 2.0	465	53
Fos-p1, pH 7.0	485	4.5
Lys 16 → Nle, pH 7.0	490	2.5
Lys 30 → Nle, pH 7.0	495	1.8
Lys 16/Lys 30 → Nle, pH 7.0	485	2.6

[a] ANS binding to proteins is accompanied by a significant increase in ANS emission intensity and a decrease in emission wavelength from 500 nm to approximately 470 nm (*51*−*53*). Such large changes in ANS fluorescence are induced by the pH 2 molten globule form of α-lactalbumin, in accord with previous results (*53*). In contrast, such large changes in ANS fluorescence are not induced by the Fos leucine zipper peptides. Experiments were performed at 5 °C.

In accord with previously published results (*17*), CD indicates that Fos-p1 is helical (Figure 2), and the molecular mass determined by sedimentation equilibrium indicates that Fos-p1 is dimeric at micromolar concentrations and 5 °C (expected mass for the dimer, 9218 Da; observed, 9100 ± 500 Da). Fos-p1 is relatively unstable, with a T_m of 30 °C at a total peptide concentration of 10 μM (Figure 3).

The thermal melting curve of Fos-p1 is sigmoidal (Figure 3), and Fos-p1 does not bind ANS (Table 1). These results suggest that the Fos-p1 dimer adopts a well-packed structure typical of native proteins. In contrast, molten globules and many designed proteins that lack structural uniqueness exhibit linear unfolding transitions and bind ANS (*26*, *42*, *43*).

The Lys 16 → Nle variant is helical (Figure 2) with a higher thermal stability than Fos-p1; the T_m at 10 μM peptide concentration is 46 °C (Figure 3).[2] The sigmoidal thermal unfolding curve (Figure 3) and lack of ANS binding (Table 1) suggest that the Lys 16 → Nle variant adopts a well-packed structure typical of native proteins.

The apparent molecular mass of the Lys 16 → Nle variant determined from individual fits of the six sedimentation equilibrium data sets is 10.9 ± 0.4 kDa, which is 19% higher than expected for a dimer (9188 Da) and 21% lower than expected for a trimer (13782 Da). The apparent mass obtained from a global fit to a single-species model is 11.1 kDa (variance = 1.4). Of various models, the sedimentation equilibrium data are best accounted for by a dimer−tetramer equilibrium as judged by the distribution of the residuals for fits to individual data sets (Figure 4). In addition, the variance, which approaches 1 as the fit improves, of a global fit of the six data sets is lowest for the dimer−tetramer model at 1.06. Significant deviations of residuals are observed for fits to models other than dimer−tetramer (Figure 4), and higher variances are seen for global fits to other possible models such as single-species trimer (variance = 13.0) and monomer−tetramer (variance = 2.76). The distribution of the residuals (Figure 4) and the variance of the global fit at 1.11 for the monomer−trimer model are only slightly less

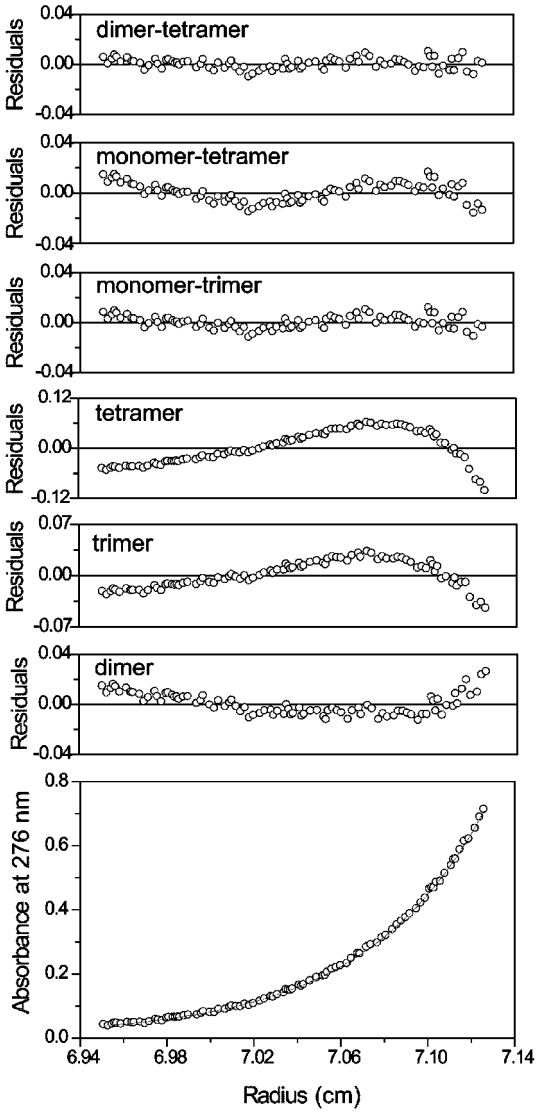

FIGURE 4: Sedimentation equilibrium data for the Lys 16 → Nle variant (PBS, pH 7.0, 5 °C, 35 krpm, total peptide concentration 140 μM). Of various models, the distribution of residuals to individual fits and variances of the global fits (see text) indicate that the data are best accounted for by a dimer−tetramer equilibrium. The apparent dissociation constant for the dimer−tetramer equilibrium is 1.0 ± 0.2 mM, and so the Lys 16 → Nle variant is predominantly dimeric at low micromolar concentrations.

[2] Measurement by urea denaturation of the changes in the free energy of unfolding due to the Nle substitutions were precluded by the lack of folded baselines at 5 °C and 10 μM peptide concentration for Fos-p1 and the Lys 16 → Nle variant and an unfolded baseline for the Lys 16/Lys 30 → Nle variant. However, the midpoints of urea denaturation for Fos-p1, Lys 16 → Nle, and Lys 16/Lys 30 → Nle are approximately 1.6−1.8, 3−3.4, and 7.6−8 M, respectively, indicating an increase in resistance to urea denaturation that parallels the increase in thermal stability upon the Nle substitutions.

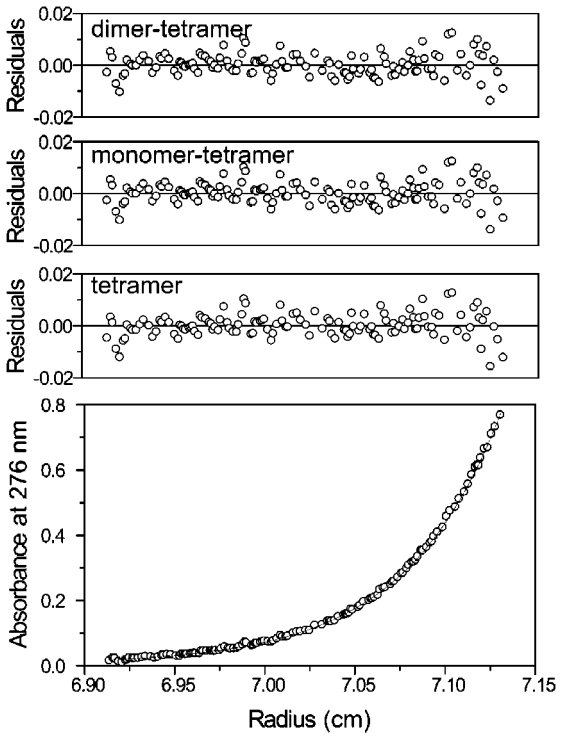

FIGURE 5: Sedimentation equilibrium data for the Lys 30 → Nle variant (PBS, pH 7.0, 5 °C, 35 krpm, total peptide concentration 140 μM). The quality of fits to various models involving the tetramer indicates that the Lys 30 → Nle variant is essentially tetrameric.

favorable than for the dimer−tetramer model (variance = 1.06). However, the thermal denaturation behavior of the Lys 16 → Nle variant is inconsistent with the presence of unfolded monomers (see Figure 2 legend) and, therefore, inconsistent with equilibria involving monomeric peptides that are likely to be largely unfolded. The Lys 16 → Nle variant therefore exists in a mixture of oligomerization states and is predominantly dimeric (>80%, assuming that the apparent mass reflects the weight-average distribution of the dimer and tetramer).

Substitution of Lys 30 with Nle results in a helical structure (Figure 2) of significantly higher thermal stability; the T_m is increased to 60 °C (Figure 3).[2] The sigmoidal thermal unfolding curve (Figure 3) and lack of ANS binding (Table 1) suggest that the Lys 30 → Nle variant adopts a well-packed structure typical of native proteins.

The apparent molecular mass of the Lys 30 → Nle variant determined from a single-species fit of sedimentation equilibrium data is 17.6 ± 0.4 kDa (data not shown). The mass obtained from a global fit of the six data sets is also 17.6 kDa, and the variance of the global fit is 1.4. These apparent masses are significantly higher than expected for a trimer (13782 Da) and approximately 4% lower than expected for a tetramer (18376 Da). The single-species tetramer (variance = 1.47), monomer−tetramer (variance = 1.52), and dimer−tetramer (variance = 1.47) models provide essentially equivalent descriptions of the data (Figure 5), and a systematic change in apparent mass with loading concentration is not observed. The sedimentation equilibrium data therefore indicate that the Lys 30 → Nle variant is essentially tetrameric.

Simultaneous substitution of Lys 16 and Lys 30 with Nle results in a helical structure (Figure 2) with increased thermal

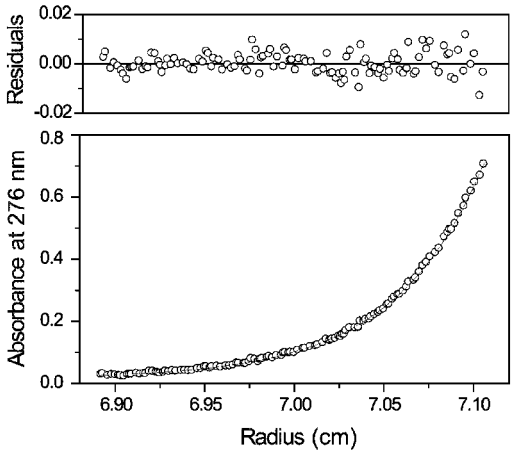

FIGURE 6: Sedimentation equilibrium indicates that the Lys 16/Lys 30 → Nle variant is tetrameric (PBS, pH 7.0, 5 °C, 35 krpm, total peptide concentration 140 μM). The random distribution of residuals indicates that a single-species tetramer accounts for data.

stability relative to the Lys 30 → Nle variant (T_m = 80 °C; Figure 3).[2] The molecular mass determined by sedimentation equilibrium indicates that the double variant is tetrameric (Figure 6). The average molecular mass obtained from individual fits of the six data sets is 18.5 ± 0.7 kDa, and the mass obtained from a global fit of all six data sets is 18.7 kDa (variance = 1.7). The expected mass for the tetramer is 18316 Da. The Lys 16/Lys 30 → Nle variant exhibits the native-like properties of a sigmoidal unfolding curve (Figure 3) and lack of ANS binding (Table 1).

The variant Fos peptides exhibit differences in $[\theta]_{222}$ at low temperatures that are unrelated to T_m. If $[\theta]_{222}$ reflects helix content only, then the Lys 30 → Nle variant is apparently less helical than Fos-p1 at low temperatures but has a higher T_m than Fos-p1, and the Lys 16/Lys 30 → Nle variant is slightly less helical than the Lys 16 → Nle variant at low temperatures but has a higher T_m than Lys 16 → Nle (Figure 3). The reason for this behavior is unclear and is seen with peptides that have been once and twice purified by C_{18} HPLC with shallow (0.1% per minute) gradients, making the presence of impurities unlikely. The values of $[\theta]_{222}$ may reflect an aromatic contribution from Tyr 40 to the CD spectra (*44*). Tyr 40 is at the C-terminal, a position in each of the Fos peptides and may be sensitive to conformational changes or oligomerization switches due to the Nle substitutions. Tyr 40 of each peptide is, however, largely solvent exposed since the fluorescence emission maximum of each peptide and of the free amino acid L-Tyr is 303 nm (PBS, pH 7.0; data not shown), as expected for a solvent-exposed Tyr (*45*). The differences in $[\theta]_{222}$ at low temperature may also reflect local unfolding of the Fos variant coiled coils, as seen for a variant GCN4 coiled coil (*46*). The presence of folded baselines for the three variant peptides suggests the absence of an equilibrium between globally unfolded and folded peptides (*46*).

DISCUSSION

Coiled coils form a widespread protein oligomerization motif (*1*, *2*), with over 5% of all putative open reading frames predicted to contain coiled-coil domains (*3*). The hallmark sequence feature of the motif, the a−d hydrophobic repeat (*4*, *5*), is a useful predictor of putative coiled coils (*4*, *5*,

10−*15*). Since the helices of coiled coils can adopt multiple oligomerization states in homo- and heteromeric complexes (*1*, *2*), it is desirable to identify sequence features that identify oligmerization orders and partners of coiled-coil assemblies.

Buried polar residues can dictate the specificity of coiled-coil oligomerization and association (*6*, *7*, *25*−*35*). For example, Asn residues at position a are a common feature of two-stranded coiled coils (*10*−*13*, *15*), including the c-Jun homodimer (*25*). In several natural and designed coiled coils, Asn at position a imparts specificity for dimerization (*7*, *25*−*29*, *33*, *47*, *48*) and helix orientation (*26*, *30*), presumably by destabilizing alternative conformations in which the hydrogen-bonding potential of the Asn side chain is unsatisfied (*26*, *48*).

Lys is a relatively common buried polar residue in coiled coils. Position a Lys residues are significantly more common in dimeric than trimeric coiled coils (*10*, *13*, *15*). A position a Lys directs formation of dimers in the context of the GCN4 coiled coil, and analysis of GCN4 coiled-coil structures suggests that the oligomerization preference may be due to preferential solvation of the Lys ϵ-amino group in the dimer relative to the trimer (*28*). Indirect evidence for a contribution of position a Lys to oligomerization specificity comes from studies of a designed coiled coil in which two peptides are cross-linked with a disulfide bond (*33*). In this context, Lys at position a decreases the stability of the dimer without resulting in an oligomerization switch (*33*). Taken together, these findings suggest that position a Lys residues promote dimer formation.

Fos forms a homodimer at micromolar concentrations but does not have a position a Asn. There are, however, two position a Lys residues. Our results indicate that dimerization of the Fos leucine zipper is mediated by Lys 30, since replacement of Lys 30 with Nle results in tetramer formation. Lys 16, in contrast, does not impart dimerization specificity to the same extent, since the Lys 16 → Nle variant is predominantly dimeric at micromolar concentrations. Simultaneous replacement of Lys 16 and Lys 30 with Nle results in a very stable homotetramer. Thus, Lys 30 plays a central role in imparting dimerization specificity to Fos at the expense of stability.

The different effects of Lys 16 and Lys 30 on oligomerization specificity indicate that the effects of position a Lys residues on coiled-coil assembly are context dependent. The influence of context may reflect different ionic interactions of the ϵ-amino groups of the two Lys residues. In the parallel Fos homodimer, Lys 30 has the potential to form an interhelical g′ → a polar interaction with a g′ position Glu of the preceding heptad of the opposing helix (Figure 1A). Such interactions are seen in the crystal structure of the parallel Fos−Jun coiled-coil heterodimer (*18*) and may contribute to dimerization specificity. In contrast, Lys 16 in an analogous g′ → a interaction would be paired with a g′ position Lys of the opposing helix (Figure 1A), which is expected to be destabilizing (*49*, *50*). Instead, Lys 16 could form an intrahelical electrostatic interaction with an e position Glu of the preceding heptad (Figure 1A), as seen in the crystal structure of a GCN4 variant with a Lys at position a (*28*). Such intrahelical interactions may not discriminate between alternative quaternary assemblies such as dimers, trimers, and tetramers, which have different interhelical packing arrangements (*7*, *8*).

Interhelical electrostatic interactions provide a mechanism to impart homo- and heteroassociation specificity (*16*, *23*, *49*). Fos homodimers are destabilized by the juxtaposition of Glu residues that form unfavorable interhelical g′ → e electrostatic interactions in the homodimer (*22*−*24*). We find that the destabilization of the Fos homodimer by unfavorable electrostatic interhelical g′ → e interactions can be alleviated, however, by an oligomerization switch to the homotetramer. The results reveal an additional facet to the mechanism of Fos destabilization, which is the role of dimerization mediated by the position a Lys residues, in placing like-charged residues in the correct context to disfavor self-association by Fos. Since Fos−Jun dimerization is driven by the instability of the Fos homodimer (*23*), imparting specificity for Fos dimerization is a key element of the molecular basis of the specificity of the Fos−Jun protein−protein interaction.

ACKNOWLEDGMENT

We thank Peter S. Kim for a gift of Fos-p1 used in the initial stages of this study and Alan J. Kennan for use of the CD spectrometer and useful discussions.

REFERENCES

1. Lupas, A. (1996) *Trends Biol. Sci. 21*, 375−382.
2. Burkhard, P., Stetefeld, J., and Strelkov, S. V. (2001) *Trends Cell Biol. 11*, 82−88.
3. Newman, J. R. S., Wolf, E., and Kim, P. S. (2000) *Proc. Natl. Acad. Sci. U.S.A. 97*, 13203−13208.
4. McLachlan, A. D., and Stewart, M. (1975) *J. Mol. Biol. 98*, 293−304.
5. Stone, D., Sodek, J., Johnson, P., and Smillie, L. B. (1975) in *Proteins of Contractile Systems* (Biro, E. N. A., Ed.) pp 125−136, North-Holland, Amsterdam.
6. O'Shea, E. K., Klemm, J. D., Kim, P. S., and Alber, T. A. (1991) *Science 254*, 539−544.
7. Harbury, P. B., Zhang, T., Kim, P. S., and Alber, T. (1993) *Science 262*, 1401−1407.
8. Harbury, P. B., Kim, P. S., and Alber, T. (1994) *Nature 371*, 80−83.
9. Parry, D. A. D. (1982) *Biosci. Rep. 2*, 1017−1024.
10. Conway, J. F., and Parry, D. A. D. (1990) *Int. J. Biol. Macromol. 12*, 328−334.
11. Lupas, L., Van Dyke, M., and Stock, J. (1991) *Science 252*, 1162−1164.
12. Berger, B., Wilson, D. B., Tonchev, T., Milla, M., and Kim, P. S. (1995) *Proc. Natl. Acad. Sci. U.S.A. 92*, 8259−8263.
13. Woolfson, D. N., and Alber, T. (1995) *Protein Sci. 4*, 1596−1607.
14. Wolf, E., Kim, P. S., and Berger, B. (1997) *Protein Sci. 6*, 1179−1189.
15. Walshaw, J., and Woolfson, D. N. (2001) *J. Mol. Biol. 307*, 1427−1450.
16. Lumb, K. J., and Kim, P. S. (1996) *Science 271*, 1137−1138.
17. O'Shea, E. K., Rutkowski, R., Stafford, W. F., and Kim, P. S. (1989) *Science 245*, 646−648.
18. Glover, J. N. M., and Harrison, S. C. (1995) *Nature 373*, 257−261.
19. Karin, M., Liu, Z., and Zandi, E. (1997) *Curr. Opin. Cell Biol. 9*, 240−246.
20. Jochum, W., Passegué, E., and Wagner, E. F. (2001) *Oncogene 20*, 2401−2412.
21. Shaulian, E., and Karin, M. (2001) *Oncogene 20*, 2390−2400.
22. Nicklin, M. J. H., and Casari, G. (1991) *Oncogene 6*, 173−179.
23. O'Shea, E. K., Rutkowski, R., and Kim, P. S. (1992) *Cell 66*, 699−708.
24. John, M., Briand, J., Granger-Schnarr, M., and Schnarr, M. (1994) *J. Biol. Chem. 269*, 16247−16253.

25. Junius, F. K., Mackay, J. P., Bubb, W. A., Jensen, S. A., Weiss, A. S., and King, G. F. (1995) *Biochemistry 34*, 6164−6174.
26. Lumb, K. J., and Kim, P. S. (1995) *Biochemistry 34*, 8642−8648.
27. Gonzalez, L., Brown, R. A., Richardson, D., and Alber, T. (1996) *Nat. Struct. Biol. 3*, 1002−1009.
28. Gonzalez, L., Woolfson, D. N., and Alber, T. (1996) *Nat. Struct. Biol. 3*, 1011−1018.
29. Zeng, X., Herndon, A. M., and Hu, J. C. (1997) *Proc. Natl. Acad. Sci. U.S.A. 94*, 3673−3678.
30. Oakley, M. G., and Kim, P. S. (1998) *Biochemistry 37*, 12603−12610.
31. Suzuki, K., Yamada, T., and Tanaka, T. (1999) *Biochemistry 38*, 1751−1756.
32. Wagschal, K., Tripet, B., and Hodges, R. S. (1999) *J. Mol. Biol. 285*, 785−803.
33. Wagschal, K., Tripet, B., Lavigne, P., Mant, C., and Hodges, R. S. (1999) *Protein Sci. 8*, 2312−2329.
34. Zhu, H., Celinski, S. A., Scholtz, J. M., and Hu, J. C. (2000) *J. Mol. Biol. 300*, 1377−1387.
35. Akey, D. L., Malashkevich, V. N., and Kim, P. S. (2001) *Biochemistry 40*, 6352−6360.
36. Porte, D., Oertel-Buchheit, P., Granger-Schnarr, M., and Schnarr, M. (1995) *J. Biol. Chem. 270*, 22721−22730.
37. Schnölzer, M., Alewood, P., Jones, A., Alewood, D., and Kent, S. B. H. (1992) *Int. J. Pept. Protein Res. 40*, 180−193.
38. Edelhoch, H. (1967) *Biochemistry 6*, 1948−1954.
39. Cantor, C. R., and Schimmel, P. R. (1980) *Biophysical Chemistry*, Freeman, New York.
40. Laue, T. M., Shah, B. D., Ridgeway, T. M., and Pelletier, S. L. (1992) in *Analytical Ultracentrifugation in Biochemistry and Polymer Science* (Harding, S. E., Rowe, A. J., and Horton, J. C., Eds.) pp 90−125, The Royal Society of Chemistry, Cambridge.
41. van Straaten, F., Muller, R., Curran, T., van Beveren, C., and Verma, I. M. (1983) *Proc. Natl. Acad. Sci. U.S.A. 80*, 3183−3187.
42. Kuwajima, K. (1989) *Proteins 6*, 87−103.
43. Betz, S. F., Raleigh, D. P., and DeGrado, W. F. (1993) *Curr. Opin. Struct. Biol. 3*, 601−610.
44. Woody, R. W., and Dunker, A. K. (1996) in *Circular Dichroism and the Conformational Analysis of Biomolecules* (Fasman, G. D., Ed.) pp 109−157, Plenum Press, New York.
45. Creighton, T. E. (1993) *Proteins: Structures and Molecular Properties*, 2nd ed., W. H. Freeman and Co., New York.
46. Lumb, K. J., Carr, C. M., and Kim, P. S. (1994) *Biochemistry 33*, 7361−7367.
47. Tanford, C. (1962) *Adv. Protein Chem. 17*, 69−165.
48. Betz, S., Fairman, R., O'Neil, K., Lear, J., and DeGrado, W. (1995) *Philos. Tran. R. Soc. London B 348*, 81−88.
49. O'Shea, E. K., Lumb, K. J., and Kim, P. S. (1993) *Curr. Biol. 3*, 658−667.
50. Vinson, C. R., Hai, T., and Boyd, S. M. (1993) *Genes Dev. 7*, 1047−1058.
51. Stryer, L. (1965) *J. Mol. Biol. 13*, 482−495.
52. Goto, Y., and Fink, A. L. (1989) *Biochemistry 28*, 945−952.
53. Semisotnov, G. V., Rodionova, N. A., Razgulyaev, O. I., Uversky, V. N., Gripas, A. F., and Gilmanshin, R. I. (1991) *Biopolymers 31*, 119−128.

BI0159276